ISSN1027-5495. Functional Materials, 31, No.4 (2024), p. 457-473
doi:http://dx.doi.org/10.15407/fm31.04.457

Recent advances in the photocatalytic remediation of polycyclic aromatic hydrocarbons

A. Timonina, I. Shcherbakov, K. Belikov, T. Shcherbakova

Institute of Functional Materials Chemistry, State Scientific Institution "Institute for Single Crystals" of NAS of Ukraine, 60 Nauky ave., Kharkiv, 61072, Ukraine

Received September 10, 2024

Polycyclic aromatic hydrocarbons (PAHs) are among the most hazardous environmental pollutants due to their high toxicity, carcinogenicity, and ability to accumulate in ecosystems. The development of effective methods for their deactivation is an extremely pressing issue in modern science. One of the most promising methods for efficient PAHs destruction is photocatalytic degradation, which is based on the use of semiconductor materials. Photocatalysis is an environmentally friendly and energy-efficient approach that facilitates the oxidation of PAHs through light irradiation, resulting in the formation of less harmful compounds. This area of research is rapidly advancing, with new materials and approaches emerging each year to enhance the efficiency of photocatalytic degradation of organic pollutants, particularly PAHs. Special attention is given to the development of new photocatalytic materials such as modified oxides of titanium, zinc, iron, and metal- and graphene-based nanocomposites, which offer high activity, stability, and effectiveness in real-world conditions. The review presented in this paper systematizes recent advancements in the field of photocatalytic degradation of PAHs, focusing on key aspects of mechanisms, materials, and future research prospects.

Keywords: PAHs, photocatalysis, nanomaterials, surface chemistry, GC-MS

Сучасні досягнення у фотокаталітичній ремедіації поліциклічних ароматичних вуглеводнів. *А. Тімоніна, І. Щербаков, Т. Щербакова, К. Беліков*

Поліциклічні ароматичні вуглеводні (ПАВ) є одними з найбільш небезпечних забруднювачів навколишнього середовища через їх високу токсичність, канцерогенність та здатність накопичуватися в екосистемах. Розробка ефективних методів їх дезактивації є надзвичайно актуальною проблемою сучасної науки. Одним із найперспективніших методів ефективної деструкції ПАВ є фотокаталітична деградація, яка базується на використанні напівпровідникових матеріалів. Фотокаталіз є екологічно безпечним та енергоефективним підходом, що забезпечує окислення ПАВ за допомогою світлового випромінювання з утворенням менш небезпечних сполук. Ця галузь досліджень активно розвивається, і з кожним роком з'являються нові матеріали та підходи до підвищення ефективності процесу фотокаталітичної деструкції органічних забруднювачів, зокрема ПАВ. Особлива увага приділяється створенню нових фотокаталітичних матеріалів, таких як модифіковані оксиди титану, цинку, заліза, нанокомпозити на основі металів і графену, які забезпечують високу активність, стабільність та ефективність у реальних умовах. Огляд, представлений у даній роботі, систематизує останні досягнення в галузі фотокаталітичної деградації ПАВ, зосереджуючи увагу на ключових аспектах механізмів, матеріалів та перспектив подальших досліджень.

1. Introduction

Polycyclic aromatic hydrocarbons (PAHs) are a large group of diverse organic compounds and are of significant attention in environmental and health studies because of their omnipresence in natural and anthropogenic sources as well as their potential adverse effects on ecosystems and human health. These compounds are generated through the incomplete combustion of organic materials and are found in various environmental matrices, including air, water, soil, and sediments [1,2]. The properties inherent to PAHs, such as heterocyclic aromatic ring structures, hydrophobicity, and thermal stability, make them highly persistent in the environment.

Despite numerous studies proving that PAHs cause carcinogenic and mutagenic effects and act as potent immunosuppressants [3], their impact on human physiological systems, particularly the cardiovascular system, has clear parallels with the growing list of non-respiratory effects associated with air pollution over the last decade [4]. They easily dissolve in fatty tissues and bioaccumulate in high concentrations in aquatic organisms, thereby exerting various hazardous and lethal effects. As PAHs are persistent pollutants posing diverse biological hazards due to their inherent characteristics, their removal has become a pressing global issue.

Although there are over 100 different types of PAHs, only benzo[a]pyrene has been recognized by the International Agency for Research on Cancer as carcinogenic [5] and overall hazardous for humans [6]. Among national authorities, only the European Union has adopted several regulations to control the content of PAHs in various environmental and consumer products as EU 2020/1255 [7] and 2023/915 [8]. In the USA, the Environmental Protection Agency under the National Primary Drinking Water Regulations [9] established a maximum permissible level of 0.2 μg/L only for benz[a]pyrene in drinking water while listing 16 PAHs as priority pollutants due to their negative impact on the environment and human health [10]. In contrast, Health Canada has not regulated PAH content in water but has established a legal limit of 3 μg/kg for benzo[a]pyrene only in olive oil products [11].

As water is recognized as a vital resource on our planet, its quality has recently garnered significant attention from both international and local authorities, leading to the adoption of strict regulations. The growing number of human-induced pollutants makes the natural sources of water increasingly vulnerable. In this context, the implementation of purification procedures before discharging polluted water back into natural resources is now a top priority for water treatment services.

PAHs contamination of aquatic ecosystems generally occurs from two main sources: anthropogenic and environmental [12]. Natural sources of PAHs pollution in aquatic ecosystems

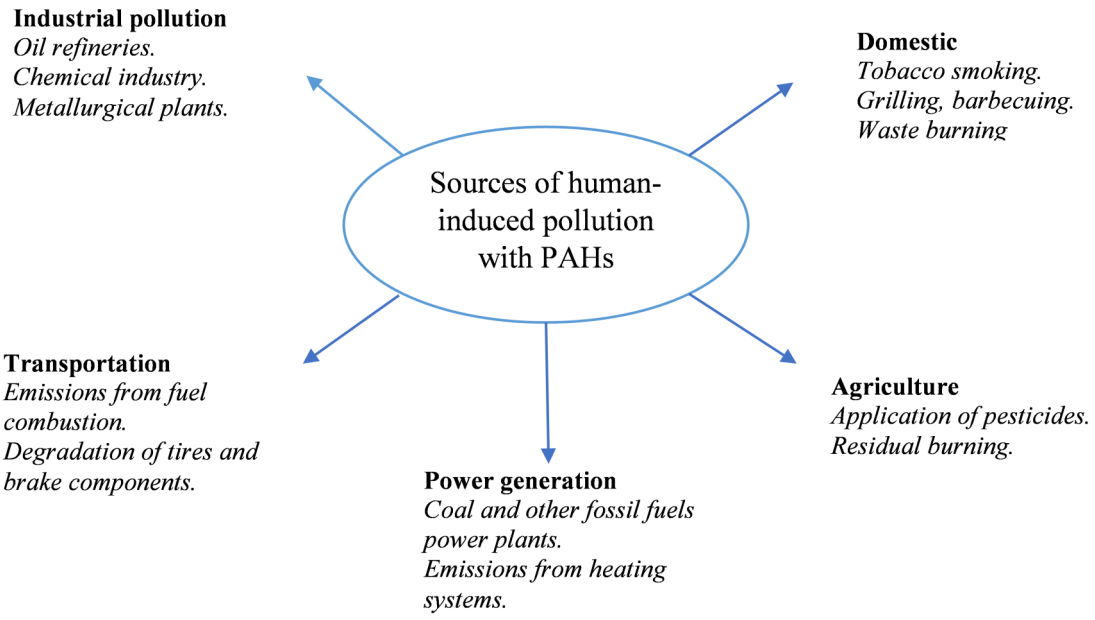

Fig. 1. Environmental anthropogenic origins of PAHs.

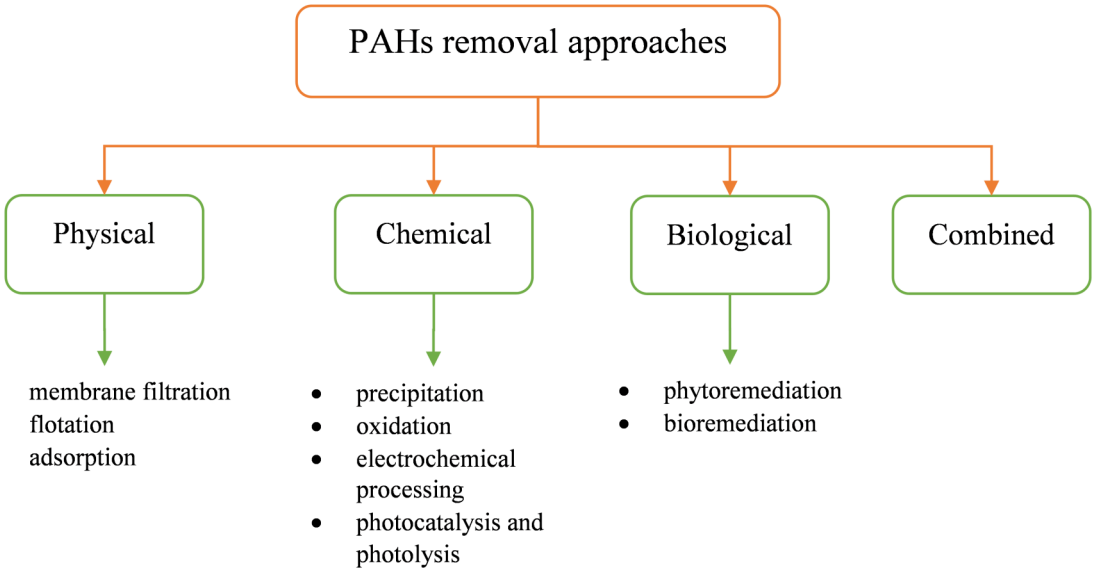

Fig. 2. Various methods for removing PAHs from wastewater.

include forest fires, peat fires, and volcanic eruptions[13]. The primary factors of anthropogenic PAHs pollution in aquatic ecosystems typically include five different types of emissions: transportation, industry, households, agriculture, and the energy sector [14–16] (Fig. 1).

To date, several technologies (Fig. 2) have been developed to combat pollutants in wastewater, including complexation, advanced oxidation, biological treatment, and adsorption [17–19]. Finding a single treatment method that effectively removes all types of organic pollutants is a challenging task due to the complexity and diversity of the organic chemicals used.

Traditional wastewater treatment techniques are often energy-intensive and therefore unsuitable for 'green' and environmentally sustainable cleaning approaches. The use of non-destructive physical methods, such as filtration, reverse osmosis, and adsorption on activated carbon, can cause secondary pollution as contaminants are merely transferred to other media [20]. Biological treatment systems face issues such as instability, low removal efficiency, high cost, and resistance to biodegradation of many chemical compounds. Additionally, some advanced oxidation processes require excessive energy expenditure during homogeneous phase operations and large amounts of oxidants, complicating their large-scale application.

Regarding PAHs, depending on the structural features and the number of benzene rings in the compounds, specifically by molecular weight they are divided into two groups: high-molecular-weight PAHs (e.g., pyrene, dibenz[a,h]anthracene, benzo[a]pyrene, chrysene), which have four or more aromatic rings, and low-molecular-weight PAHs (e.g., naphthalene, acenaphthene, fluorene, phenanthrene), which have two or three aromatic rings. As molecular weight increases, these compounds are released into the environment as gaseous and solid particles [21]. The general structure of PAHs is aromatic with very high π-electron density, which accounts for their high thermodynamic stability and resistance to nucleophilic attack. High-molecular-weight PAHs tend to decrease in water solubility and increase in lipophilicity, making them more difficult to dissolve [22]. Due to these properties, the traditional wastewater treatment approaches are ineffective against PAHs, prompting researchers to seek alternative destruction technologies that ensure the removal of such stable organic pollutants. These approaches include ultraviolet light processes, membrane-based processes, and advanced oxidation processes [23,24].

According to a comparative analysis of these methods, heterogeneous photocatalysis has been recognized as a promising and environmentally friendly method for removing many persistent organic pollutants from various media. This method attracts attention due to its high efficiency, low cost, and ease of implementation [25]. It involves the photon-stimulated advanced oxidation of hazardous organic pollutants, resulting in environmentally safe by-products under favorable temperature conditions with minimal external energy input [26]. The oxidation reaction of organic pollutants oc-

curs at room temperature using a cheap, harmless catalyst that can be reused. Finally, this technique allows for the treatment of hazardous pollutants that may be present in complex mixtures with other organic compounds [27].

However, PAHs still present a significant challenge for researchers to find an effective approach to degrade them into harmless products. This is evidenced by search queries in the Web of Science Core Collection (Fig. 3). While the topics 'Polycyclic Aromatic Hydrocarbons' and 'polycyclic aromatic hydrocarbons degradation' return 81K and 11K records respectively, the specified 'polycyclic aromatic hydrocarbons photocatalytic degradation' returns only 397 records, proving photocatalysis to be a relatively new approach for PAHs removal.

Moreover, if the data from the last two requests are compared, one can observe that the topic 'polycyclic aromatic hydrocarbons degradation' was on a rising trend from the early 2010s, with a slight decrease in the last three years while the topic 'polycyclic aromatic hydrocarbons photocatalysis degradation' shows a gradual increase over time (Fig. 4).

This review aims to provide a comprehensive overview of recent advanced in the degradation of polycyclic aromatic hydrocarbons through photocatalysis, highlighting the latest advancements, challenges, and future directions in this field. By synthesizing current research, authors aimed to offer valuable insights for the scientific community working towards effective PAHs remediation strategies.

2. Mechanism of photocatalytic degradation of PAHs

In recent decades, there has been a significant increase in research activity in the fields of nanoscience and nanotechnology. When the size of a material is reduced to the nanometer scale, the new physical and chemical properties emerge. The properties of nanomaterials also change with their shape [28]. Among the unique characteristics of nanomaterials, it is noteworthy that the movement of electrons and holes in semiconductor nanomaterials is predominantly regulated by quantum confinement. The transport properties associated with phonons and photons are significantly influenced by the size and geometry of the materials. The specific surface area and surface-to-volume ratio increase substantially as the material size decreases [29]. Due to their smaller size, nanoparticles have a significantly larger surface area, which

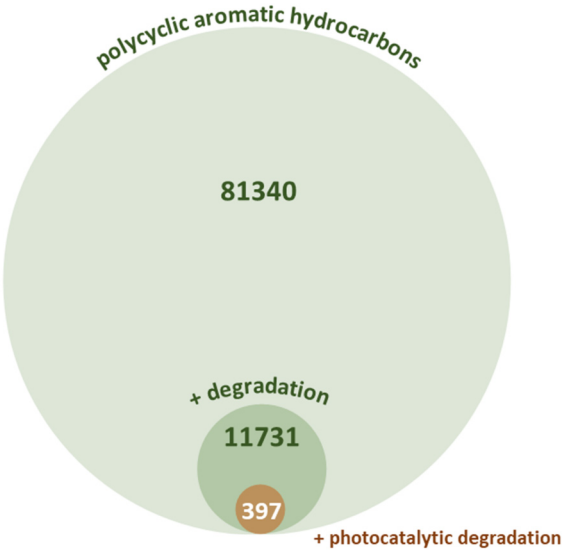

Fig. 3. Reference record count from Web of Science Core Collection for 'Polycyclic Aromatic Hydrocarbons', 'polycyclic aromatic hydrocarbons degradation' and 'polycyclic aromatic hydrocarbons photocatalytic degradation' search requests.

enhances the surface chemical effect of the nanoparticles, allowing chemical reactions to occur on their surface [30].

Heterogeneous photocatalysis is a process that is actively researched as a promising method for the removal of persistent organic pollutants from water and air. Heterogeneous photocatalysis involves the use of a photoactive material (solid photocatalyst), usually a semiconductor material, which is excited upon light irradiation, generating electron-hole pairs that can ultimately participate in various chemical reactions [31].

The primary mechanism of the process involves:

Photon Absorption: The process begins with the absorption of photons with energy equal to or greater than the bandgap energy of the semiconductor. This leads to the excitation of an electron (e^-) from the valence band to the conduction band, leaving behind a hole (h^+) in the valence band.

$$catalyst + h\nu \rightarrow e^- + h^+ \quad (1)$$

Here $h\nu$ is the photon of light, e^- is an excited electron and h^+ is a hole.

Generation of Electron-Hole Pairs. The excited electron (e^-) and hole (h^+) can recombine, releasing the absorbed light energy as heat, without initiating any chemical reaction. Alternatively, they can participate in redox reactions with adsorbed substances, as the valence band

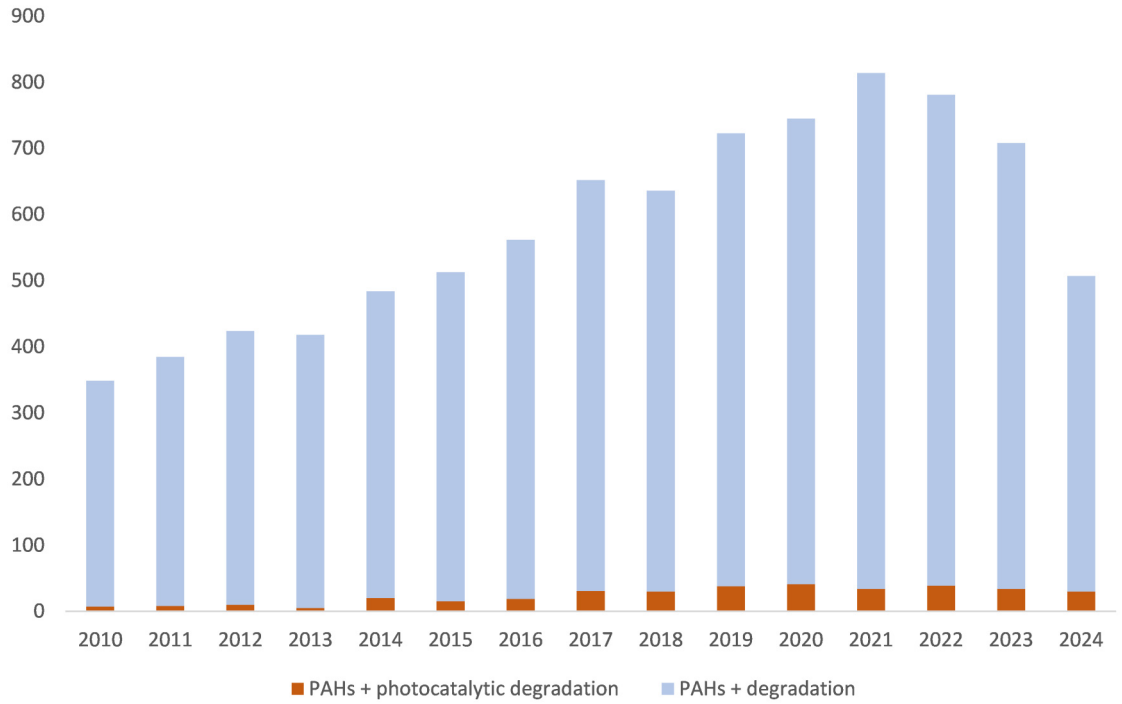

Fig. 4. Number of reference records count per year in Web of Science Core Collection for various requests related to PAHs.

hole (h^+) is highly oxidative, and the conduction band electron (e^-) is highly reductive. On the semiconductor surface, the excited e^- and h^+ can engage in redox reactions with water, hydroxide ions (OH^-), organic compounds, or oxygen, leading to the mineralization of the pollutant.

Reactions with Water and OH^- Groups.

The hole (h^+) in the valence band can interact with water molecules and hydroxide ions, forming hydroxyl radicals, which are powerful oxidizing agents:

$$h^+ + H_2O \rightarrow OH^\bullet + H^+ \quad (2)$$

$$h^+ + OH^- \rightarrow HO^\bullet h^+ + OH^- \rightarrow HO^\bullet \quad (3)$$

Oxygen plays a crucial role in the photocatalytic process as it can capture electrons from the conduction band, forming superoxide radicals ($O_2^{-\bullet}$). This prevents the recombination of electron-hole pairs, thereby increasing the efficiency of the catalysis. The subsequent reactions include:

Formation of Superoxide Radicals.

$$O_2 + e^- \rightarrow O_2 \quad (4)$$

These radicals can attack PAHs, breaking down their aromatic structures and leading to the formation of various products and intermediates.

Reactions with Superoxide Radicals and Formation of Hydrogen Peroxide.

$$O_2^{-\bullet} + H^+ \rightarrow HO_2^\bullet \quad (5)$$

$$HO_2^\bullet + e^- \rightarrow HO_2^- \quad (6)$$

$$2HO_2^\bullet \rightarrow H_2O_2 + O_2 \quad (7)$$

$$2HO_2^- \rightarrow H_2O_2 + O_2 \quad (8)$$

The decomposition of hydrogen peroxide:

$$H_2O_2 + e^- \rightarrow HO^\bullet + OH^- \quad (9)$$

$$H_2O_2 + O_2^- \rightarrow HO^\bullet + OH^- + O_2 \quad (10)$$

These reactions generate hydroxyl radicals ($HO^\bullet$), which are key players in the degradation of organic pollutants [32].

An important requirement for a photocatalyst is that its bandgap energy matches the redox potential of $H_2O/ HO^\bullet(OH^- \rightarrow HO^\bullet + e$, $E_0 = -2.8V$) [33]. As the bandgap width increases in the nanometer range of particles, the energy required to overcome it also increases, shifting the effective spectral range for photocatalysis towards the ultraviolet region.

3. Key photocatalytic nanomaterials for PAHs remediation

The primary challenges for effective photocatalysis are the stability, durability, and efficiency of semiconductor photocatalysts. For practical applications, researchers strive to develop highly efficient and stable photocatalysts [34]. However, many well-known photocatalysts for PAHs cannot operate effectively under sunlight due to their wide bandgap energy (3.1 eV) and low solar energy harvesting capability (4-6%).

Nanomaterials used for the remediation of persistent organic pollutants can be classified as metallic (e.g., metal/metal oxides, carbon-based nanomaterials, nanocomposites) and non-metallic (e.g., nanomembranes, polymeric nanomaterials, metal-organic frameworks) [33].

Titanium dioxide-based nanomaterials

Titanium dioxide (TiO_2) is renowned for its chemical properties, making it extremely attractive for photocatalytic applications. It possesses high chemical stability, non-toxicity, relatively low cost, and the potential for industrial scalability. Due to its structure, TiO_2 has a wide bandgap of approximately 3.0-3.2 eV, allowing it to absorb ultraviolet radiation with wavelengths shorter than 385 nm. This makes it one of the most widely used materials for the photocatalytic purification of water from organic pollutants.

The photocatalytic activity of TiO_2 is largely determined by its crystalline phase, level of crystallinity, particle size, impurities in the crystal lattice, density of surface hydroxyl groups, and overall surface area. TiO_2 has three main crystalline phases as anatase, rutile, and brookite. While anatase and rutile exhibit similar tetragonal crystalline structures, brookite has an orthorhombic crystalline structure. These three polymorphs also have different bandgap energies, namely 3.2 eV, 3.0 eV, and 3.3 eV for anatase, rutile, and brookite, respectively [35]. The anatase phase is the most photocatalytically active [36] as it is characterized by a high concentration of surface hydroxyl groups (OH) and a significant surface area, which contribute to its enhanced photocatalytic activity compared to other phases [37,38]

The development of TiO_2-based materials has led to the design of mixed-phase titanium photocatalysts. One notable example is Degussa P25, a commercially available photocatalyst widely used in research and industry due to its unique properties. It is a mixture of anatase and rutile in a 75:25 ratio, which provides high photocatalytic activity. Anatase, with its enhanced activity, is traditionally considered the primary catalyst in P25, while rutile functions as an electron sink. Studies have shown that this mixed-phase titanium material exhibits slower charge carrier recombination rates, increased photoefficiency, and reduced activation energy under light exposure [39].

High bandgap energy is one of the main challenges in using TiO_2 as a photocatalyst as this limits its effectiveness to the UV region of the spectrum, which constitutes only about 5% of solar radiation. Such a limited absorption spectrum significantly reduces the efficiency of TiO_2 under sunlight, necessitating the additional energy expenditure for artificial lighting in industrial setups. Another serious issue of titanium oxide is its high recombination rate of electron-hole pairs, which limits the time during which the active radicals can participate in the photocatalytic reactions. This reduces the efficiency of the PAHs oxidation process and may require an increased exposure time or the addition of dopants to enhance the photocatalyst's activity [40,41].

Various strategies have been proposed to enhance the photocatalytic efficiency of TiO_2, including morphological modifications such as increasing surface area and porosity, or chemical modifications by incorporating small amounts of additional components like cations and metal oxides into the TiO_2 structure [42].

Non-Metal Doping: doping TiO_2 with nonmetals such as nitrogen (N), sulfur (S), and phosphorus (P) can reduce the bandgap energy and shift the absorption spectrum into the visible light region. This modification allows TiO_2 to utilize a broader range of the solar spectrum, thereby enhancing its photocatalytic activity.

Metal Doping: insertion of the transition metal atoms (e.g., Fe, Cu, Mn) into the TiO_2 structure also helps to reduce the bandgap energy and improve light-harvesting efficiency. Some metals can create additional active sites on the photocatalyst surface, increasing the number of generated radicals and reducing the likelihood of electron-hole pair recombination. This results in a more efficient photocatalytic process.

Graphene-based composite materials (e.g., nanosheets, quantum dots) can be integrated with TiO_2 nanostructures, resulting in synergistic properties that enhance the functionality

of the resulting composite [34]. In a study [43] , a series of TiO_2-graphene (P25-GR) composites with varying graphene (GR) content were synthesized via a hydrothermal reaction of graphene oxide (GO) and P25.

In another study [44] the relationship between the molecular structure of PAHs and their photocatalytic degradation in aqueous media was studied using Pt/TiO_2-SiO_2-based catalysts, which consist of 1% platinum particles, 20% TiO_2, and 79% silica. The study demonstrated that the degradation efficiency of PAHs varies depending on their molecular structure. For instance, highly aromatic PAHs such as benzo[a]pyrene achieved a degradation rate of 85% within 4 hours, whereas less aromatic PAHs like naphthalene had a degradation rate of 60% over the same exposure time. It was also found that PAHs with larger and more complex molecular structures exhibited slower degradation because of the difficulties in accessing the active sites of the photocatalyst. Based on the differences in the highest occupied molecular orbital energy (E_{homo}), and the lowest unoccupied molecular orbital energy (E_{lumo}) (GAP = $E_{lumo} - E_{homo}$), the authors predicted the photocatalytic degradation capability for 67 PAHs.

In a study of the photocatalytic degradation of PAHs under sunlight conditions, TiO_2@ZnHCF nanocomposite was synthesized via a two-step co-precipitation method [45]. It was found that doping TiO_2 resulted in an increased surface area (118.15 m²/g) and a reduced bandgap energy (1.65 eV). This modification demonstrated superior photocatalytic degradation results for acenaphthene (96%), phenanthrene (95%), and fluorene (93%) compared to ZnHCF (75%, 73%, 70%) and TiO_2 (55%, 50%, 47%) respectively.

A decrease in bandgap energy (2.64 eV) was observed in Cu/N-doped TiO_2 synthesized using a modified sol-gel method [46]. All photocatalyst nanoparticles belonged to the anatase phase structure with crystallite sizes ranging from 11 to 30 nm, which decreased with copper and nitrogen doping. The photocatalytic activity of Cu/N-doped TiO_2 nanoparticles was the highest compared to precursor nanoparticles (TiO_2 and N-doped TiO_2). It was also found that the efficiency of phenanthrene photodegradation under visible light was slightly higher (96%) than under UV irradiation (94%).

TiO_2/TiNTs nanocomposites, synthesized through a two-step hydrothermal treatment, were characterized by a large surface area, high content of -ONa/H groups, and a fine-crystalline anatase phase [47]. These nanocomposites demonstrated an approximately tenfold increase in the observed degradation rate constant for phenanthrene compared to unmodified TiNTs.

Synthesis of a new $BiOBr/TiO_2$-based photocatalyst modified with AgBr using a facile co-precipitation method reported in [48]. This study highlighted the enhanced photocatalytic activity of the synthesized material due to increased light absorption and charge carrier separation at the heterojunction between BiOBr and TiO_2. Additionally, AgBr with its narrow bandgap acted as a photosensitizer, enhancing light utilization and promoting the degradation process. The $BiOBr/TiO_2$ photocatalyst exhibited significantly higher activity compared to pure BiOBr and TiO_2, achieving 7.6 times higher activity compared to that of TiO_2 and 4 times higher to BiOBr under sunlight.

Zinc oxide-based photocatalysts

Zinc oxide (ZnO) is a wide-bandgap n-type semiconductor with a bandgap energy ranging from 3.2 to 3.7 eV and a large free-exciton binding energy (60 meV). The large bandgap in bulk ZnO is a drawback as it requires UV radiation to function as a photocatalyst. Unlike TiO_2 zinc oxide is chemically unstable at pH < 4, which somewhat limits its potential applications [49]. Additionally, the high recombination rate of electrons and holes results in a short carrier lifetime in pure ZnO, further hindering its implementation in photocatalytic degradation technologies.

Modification methods for ZnO are similar to those for TiO_2 and are aimed at increasing the lifetime of photogenerated electrons and holes, as well as to improve zinc oxide's ability to absorb visible light [50].

Chemical modification methods include doping with alkali metals, rare earth metals, transition metals, and non-metals, which lead to a reduction in the bandgap energy through various mechanisms [51–53]. Another potential approach to enhance the photocatalytic properties of oxide materials, including ZnO, is doping with noble metals, particularly silver. Such dopants induce the surface plasmon resonance effect, which leads to improved light absorption in the visible range and, consequently, to an increase in the photocatalytic activity of the materials.

An important and powerful strategy to enhance the photocatalytic activity of oxide

semiconductor materials is the creation of heterojunctions. Heterojunctions were a proven strategy to enhance the charge separation of electron-hole pairs, which increased the lifetime of the charge carriers as well as the redox potentials of the materials to promote various redox-based reactions [54,55]. The types of heterojunctions and examples of corresponding materials were summarized in [50].

The efficiency of photocatalytic degradation of PAHs using commercially available ZnO samples can be improved by adding oxidizing agents to the treated water. In a study [56] the authors observed a synergistic effect of ZnO and $Na_2S_2O_8$ in the photocatalytic degradation of six PAHs, with 90% of PAHs degrading within 7-15 minutes. The addition of hydrogen peroxide also enhanced the degradation degree of PAHs, particularly anthracene, when using unmodified ZnO [57].

The nanocomposite of zinc hexacyanoferrate encapsulated with zinc oxide was applied for the photocatalytic degradation of benz[a]anthracene and benzo[a]pyrene [58]. Due to the encapsulation procedure and the intercalation properties of zinc hexacyanoferrate, the specific surface area was increased, and the bandgap energy of the material was reduced, leading to improved photocatalytic activity compared to unmodified ZnO.

In some studies, authors proposed using natural components to obtain ZnO-based photocatalysts [59,60]. In one study [61] the authors obtained a core-shell nanocomposite based on zeolite and ZnO with a bandgap energy of 2.65 eV, a low recombination rate of photogenerated electron-hole pairs, and consequently, high photocatalytic activity towards PAHs.

Materials based on ZnO were also developed for air purification from PAHs present in atmospheric aerosols (particulate matter). The authors [62] developed a bifunctional hydrogel composite based on ZnO, polyacrylamide, and polyvinyl alcohol, which had a moist-looking side and a photocatalyst-embedded side. This composite exhibited high photocatalytic activity for the degradation of PAHs in particulate matter emitted from incense smoke, corn cob, and leaf litter burning under sunlight irradiation.

Other photocatalytic nanomaterials

Literature study for last five years finds there are two main nanomaterial domains as silver and silver phosphate (Ag, Ag/A_3PO_4) and iron oxides (Fe_2O_3 or Fe_3O_4) with graphene oxide (GO) and graphitic carbon nitride (g-C_3N_4)

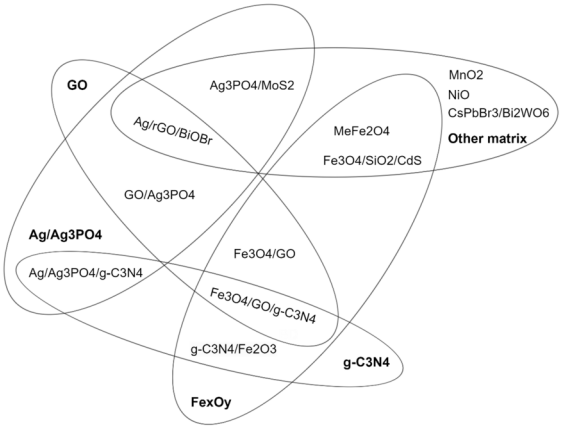

Fig. 5. Main nanomaterial domains of interest for PAHs photocatalytic degradation for past 5 years.

systems to improve the photocatalytic properties (Fig. 5), Also other oxide and non-oxides matrices like $CsPbBr_3$ or sulfides are of interest.

There has been studied the photocatalytic degradation of 3,6-dimethylphenanthrene (3,6-DMP) and phenanthrene using an Ag/rGO/BiOBr catalyst, synthesized by doping BiOBr with silver and reduced graphene oxide (rGO) [63]. Experiments were conducted under both sunlight and visible light irradiation, revealing that the degradation of 3,6-DMP was affected by solution pH, catalyst dosage, and the presence of humic acid. The catalyst showed superior performance with the optimum doping amounts Ag=1.5 wt% and rGO=3 wt% under sunlight with 3,6-DMP degrading more readily than phenanthrene. In another study [64] Dai with colleagues studied the degradation of phenanthrene with Ag/Ag_3PO_4/g-C_3N_4 heterojunction nanocomposite, created by uniformly wrapping g-C_3N_4 nanosheets around Ag_3PO_4 nanopolyhedrons. This experiment, conducted under visible light, achieved a degradation rate of 0.01756 min^{-1} for phenanthrene and maintained high activity over four cycles. Same year they also reported [65] the study where Ag_3PO_4 nanopolyhedrons were synthesized under mild conditions, and their photocatalytic properties were optimized by adjusting the Ag nanoparticle content. The composite achieved a 97.3 % removal rate of acenaphthylene under visible light, with a degradation rate of 0.03512 min^{-1}. The surface plasmon resonance of Ag nanoparticles enhanced the visible light absorption and photogenerated carrier separation, leading to high photocatalytic activity and stability over

four cycles. Wang with co-authors [66] studied the degradation of phenanthrene, pyrene, and benzo[a]pyrene using an Ag_3PO_4/MoS_2 composite catalyst with a 10% MoS_2 mass fraction. Optimal conditions, such as pH and catalyst dosage, were established, resulting in degradation rates of 99.7% for phenanthrene, 99.4% for pyrene, and 96.9% for benzo[a]pyrene, with 93.5% efficiency sustained after four cycles.

Marques [67] conducted experiments to study the photocatalytic capability of amorphous α-Fe_2O_3 to degrade PAHs. Solutions containing 16 US EPA priority PAHs were spiked with Fe_2O_3 and incubated under stable temperature (20°C) and light (9.6 W/m^{-2}) conditions for 28 days. The degradation of fluorene, phenanthrene, and benzo(a)pyrene was significant, with a photodegradation rate of 71% for benzo(a)pyrene in the presence of Fe_2O_3. However, Fe_2O_3 acted as a shield for some PAHs, hindering their photodegradation. The photocatalytic degradation of naphthalene was explored by Ali [68] with Fe_3O_4/GO/g-C_3N_4 ternary composites synthesized via co-precipitation and hydrothermal methods. This nanocomposite achieved 87.56% degradation of naphthalene in 140 minutes under visible light, outperforming both Fe_3O_4/GO and Fe_3O_4 nanomaterials. Optimal conditions included lower naphthalene concentration, higher catalyst dosage, and moderate pH. The degradation followed pseudo-first-order kinetics with a rate constant of 0.0137 min^{-1}. Al-Hunaiti [69] studied the photooxidative degradation of anthracene, phenanthrene, and naphthalene using magnetic $CrFe_2O_4$ nanoparticles under visible light LED irradiation. The $CrFe_2O_4$ nanoparticles, synthesized using Boswellia Carteri resin, showed good photocatalytic performance, achieving removal efficiencies of 99% for anthracene, 90% for phenanthrene, and 86% for naphthalene. The degradation followed first-order kinetics and the Langmuir model. A novel magnetic core-shell Fe_3O_4@SiO_2@CdS embedded graphene oxide (GO) composite was prepared by Li [70] for the visible-light-driven photodegradation of phenanthrene and pyrene. The GO-Fe_3O_4@SiO_2@CdS composite removed 86.4% of phenanthrene and 93.4% of pyrene, maintaining high photocatalytic activity over five cycles. The photocatalytic degradation of fluoranthene in soil was studied using g-C_3N_4/alpha-Fe_2O_3 [71]. The optimal degradation efficiency was 88.7% after 12 hours of simulated sunlight irradiation. The degradation followed pseudo-first-order kinetics, with center dot O_2^- and h^+ as the main active species. The coupling of g-C_3N_4 and α-Fe_2O_3 enhanced charge transport and inhibited electron-hole recombination, improving photocatalytic activity.

The photocatalytic degradation of phenanthrene was investigated by Qiao [72] using non-metallic g-C_3N_4 nanosheets under visible light. The study achieved a 100% removal efficiency of phenanthrene at initial concentration 5 mg/L within 10 minutes. Reactive oxygen species such as O_2^-, O_2, and OH were generated, with O_2^- and O_2 being the main active species. The presence of humic acid and chloride ions influenced the removal rate, while nitrate ions had no significant effect. This research offered a potential in-situ method for removing PAHs in urban river environments. The application of $CsPbBr_3$ quantum dots in study by Huang [73] was extended to the photocatalytic degradation of PAHs in tobacco tar, collected from used cigarette filters. Coupled with Bi_2WO_6, the $CsPbBr_3/Bi_2WO_6$ composite demonstrated over 96% degradation of PAHs within 50 minutes under simulated solar irradiation, showcasing its large specific surface area, excellent light absorption, and rapid charge separation. This study highlights the novel application of halide perovskite in environmental remediation. Manganese dioxide (MnO_2) was evaluated for its ability to degrade benzo(a)pyrene in aqueous solutions [74]. Nanoflower MnO_2, with a higher concentration of oxygen vacancies, showed enhanced PAHs removal by 14.28%-43.21% compared to other MnO_2 morphologies. The synergistic effects of oxygen vacancies and Mn^{3+} facilitated efficient PAHs degradation. The photocatalytic decomposition of anthracene was studied using NiO nanoparticles under ultraviolet light and sunlight [75]. The NiO nanoparticles, with sizes ranging from 37 to 126 nm, achieved 79% degradation of pyrene at 2 μg/mL of anthracene within 60 minutes. The adsorption efficiency was significant at pH=5, and the degradation followed pseudo-first-order kinetics. Additionally, authors found NiO nanoparticles were showing antimicrobial activity against Gram-negative and Gram-positive bacteria, demonstrating their dual application in bioremediation and pathogen control.

Table 1 shows the summarized data on photocatalytic degradation efficiency of various nanomaterials towards PAHs.

Table 1. Examples of typical photocatalytic nanomaterials studied recently

Material	PAHs	Testing conditions	Efficiency, %	**Ref.**
P25-TiO_2	anthracene	artificial solutions, irradiation 2.5 mW/cm^2 for 3 hrs	97	[76]
TiO_2-graphene (P25-GR) P25-2.5% composite	phenanthrene, fluoranthene, benzo[a]pyrene	artificial solutions, λ > 320 mn at 4.8 mW/cm^2 for 2 hrs	81 78 85	[43]
TiO_2@ZnHCF	acenaphthene, phenanthrene, fluorene	artificial solutions, sunlight	93–96	[45]
TiO_2/TiNTs	phenanthrene	artificial solutions, UV at λ = 365 nm for 2 hrs	93	[47]
TiO_2 doped with Cu/N	phenanthrene	artificial solutions, 300 W Xe lamp, λ > 387 nm for 2 hrs	96	[46]
TiO_2	pyrene, phenanthrene	artificial solutions, UV at λ = 365 nm for 2 hrs	92 87	[77]
TiO_2 + AgBr/BiOBr/	anthracene	artificial solutions, 300 W Xe lamp with AM 1,5 G at 95 mW/cm^2) for 10 mins	100 for 30 μg/L	[48]
TiO_2/Fe	anthracene	artificial solutions, 1 hr of irradiation	98	[78]
TiO_2/SiO_2-600 TiO_2/SiO_2-800	phenanthrene	artificial solutions, sunlight for 3 or 10 hrs	97 100	[79]
Pt-HTiO_2	naphthalene	artificial solutions, simulated sunlight for 4 hrs	82	[80]
TiO_2/Fe-1%@SiO_2	naphthalene, acenaphthene, acenaphthylene	artificial solutions, 18 W UV lamp, λ = 365 nm for 24 hrs	90 80 80	[81]
3D Printed TiO_2 Composites (3D printed PLA-TiO_2 disk)	fluoranthene, benz[a]anthracene, pyrene, benzo[a]pyrene, chrysene	artificial solutions, fluorescent lamp ReptiSun 5.0, λ (400-750 nm)=65%, λ (320-400 nm)=30%, λ (280-320 nm)=5% for 24 hrs	91 >94 >80 54 >68	[82]
TiO_2/CQDs/$CdIn_2S_4$	acenaphthylene	artificial solutions, 300 W Xe lamp, λ > 400 nm for 1 hr	88	[83]
$NiFe_2O_4$/TiO_2	naphthalene	artificial solutions, simulated sunlight for 2.5 hrs	67	[84]
ZnO	benzo[a]pyrene, benzo[b]fluoranthene, benzo[ghi]perylene, benzo[k]fluoranthene, fluoranthene, indene[1,2,3-cd]pyrene	groundwater, natural sunlight for 50 min 120 50 min 360 min 50 min 50 min	100	[56]
ZnO	anthracene	aqueous ethanol model solution, λ = 254 nm and 368 nm for 280 min	80	[57]
		model emulsion solution, λ = 254 nm, 368 nm for 230 min	90	
ZnHCF@ZnO	benz[a]anthracene benzo[a]pyrene	artificial solutions, natural sunlight	93 90	[58]
GO/ZnO	phenanthrene	artificial solutions, UV–Vis for 120 min	86-96	[60]

ZA@ZnO_{1-X}	fluorene phenanthrene anthracene	artificial solutions, 300 W halogen lamp for 120 mins	96 95 93	[61]
Cu@ZnO	anthracene naphthalene	artificial solutions, UV irradiation	94 96	[85]
n-ZnO/p-MnO	anthracene	artificial solutions, UV at λ = 365 nm for 40 min	97	[86]
ZnO/PAM-PVA	mixture of PAHs	particulate matter, natural sunlight	13-100	[62]
Ag_3PO_4/MoS_2	pyrene, phenanthrene, benzo[a]pyrene	UV of artificial solutions	93 after 160 mins (Pyr, Phe) and 8 hrs for BaP	[66]
Fe_2O_3	fluorene, phenanthrene, benzo(a)pyrene	visible light (9.2 W/m2) irradiation of water samples	71 after 28 days	[67]
Fe_3O_4/GO/g-C_3N_4	naphthalene	visible light, pH = 5…9 of artificial solutions for 140 mins	88	[68]
$CrFe_2O_4$	anthracene, phenanthrene, naphthalene	visible LED light of artificial solutions	99 90 86	[69]
$Fe_3O_4@SiO_2@CdS$	phenanthrene, pyrene	deionized water	86 93	[70]
g-C_3N_4/α-Fe_2O_3	fluoranthene	5% catalyst in the soil-water suspensions at pH = 7, UV for 12 hrs	88	[71]
g-C_3N_4	mixture	5 mg/L of PAH, 1 g/L of g-C_3N_4	100	[72]
$CsPbBr_3$/ Bi_2WO_6	naphthalene	UV Xe lamp of tobacco tar for 50 mins	96	[73]
Ag_3PO_4	acenaphthylene	artificial solutions, UV for 2 hrs	97	[65]
NiO	anthracene, pyrene	5 pH, 60 mins UV of wastewater	79	[75]

4. Products and intermediates of photocatalytic degradation of PAHs

Under ideal conditions, the photocatalysts are activated by light of a specific wavelength, leading to the formation of electron-hole pairs that migrate to the phase boundary. These pairs generate holes and hydroxyl and superoxide radicals, which play a key role in photocatalytic oxidation. Hydroxyl radicals actively interact with aromatic hydrocarbons, leading to their hydroxylation. The peroxy radicals formed in the process further degrade PAHs by causing the cleavage of molecular rings and the formation of less toxic products such as CO_2 and H_2O. Hydroxylated intermediates and ring-opening products are more common in the initial stages of degradation, while acids, hydrocarbons, and alcohols appear in the later stages. The reaction typically initiates at the benzene fragment with the lowest localization energy. Further oxidation of PAHs intermediates leads to bond cleavage and the formation of ring structures and PAHs fragments.

The analysis of mass spectra obtained by gas chromatography/mass spectrometry (GC-MS) allowed the identification of reaction intermediates and the proposal of possible pathways for PAHs photodegradation, showcasing the stages of oxidation and breakdown of intermediates. Studies show that each compound can form several degradation products, as described in Table 2 which summarizes the information on selected PAHs and their intermediate products formed during the degradation process.

5. Real applications of PAHs remediation: floating photocatalysts?

Photocatalytic materials in powder form are often challenging to apply on a large scale and subsequently load onto a matrix for convenient

Table 2. Data on selected PAHs and their intermediates formed during degradation, identified by means of GC-MS.

PAH	Identified intermediates of heterogenous photocatalysis	**Reference**
Naphtalene	1-naphthalenol	[87,88]
	1,4-naphthoquinone	
	coumarin	
	2-hydroxynaphthoquinone	
	1,2-benzenedicarboxaldehyde	
	1,2-benzenedicarboxylic acid	
	2-hydroxybenzaldehyde	
	2,3-dihydroxybenzaldehyde	
	hydroquinone	
	acetic acid	
	oxalic acid	
	methanol	
Acenaphthylene	1-acenaphthenol	[88]
	acenaphthenone	
	acenaphthylenedione	
	1H,3H-naphtho(1,8-cd) pyran-1-one	
	1,8-naphthalic anhydride	
Phenanthrene	9-phenanthrenol	[89]
	phenanthro[9,10-b]oxirene	
	9,10-phenanthrenedione	
	diethyl phthalate	
	2-cyclohexene-1-ol	
	2-cyclohexene-1-one	
	1,2-cyclohexanedione	
	octyl acrylate	
	2-vinyl-2-butenal	
	2-hexenal	
	5-hydroxymethyldihydrofuran-2-one	
	9-octadecanoic acid	[90]
	hexadecanoic acid	
	1-heptanol-2,4-diethyl	
	heptadecane	
	octadecane	
	9-phenanthrenol	[45]
	(1,1-biphenyl)-2,2-bicarboxaldehyde	
	benzene-1,2,3- triol	
	(Z)-4-hydroxypent-2-enedioic acid	
	(Z)-3-hydroxyacrylaldehyde	
Fluorene	9H-fluoren-9-ol	[45]
	2′-hydroxy-[1,1′-bi-phenyl]-2-carboxylic acid	
	2-hydroxybenzoic acid	
	benzene-1,2,3-triol	
	(Z)-1,4-dihydroxybut-1-ene-1,2,3,4-tetracarboxylic acid	
	(Z)-3-hydroxyacrylaldehyde	
Fluoranthene	cyclohexane(1-hexadecylheptadecyl)	[90]
	9-fluorenone	[43]
	diisopropyl phthalate	
Acenaphthene	2,3,4-trihydroxynaphthalene-1,8-dicarboxylic acid	[45]
	(2Z, 4Z)-2,3,4-trihydroxyhexa-2,4-dienedioic acid	
	(Z)-prop-1-ene-1,2,3-triol	
	3-hydroxyacrylaldehyde	

Chrysene	2-hydroxyphenanthrene-1-carboxylic acid	[91]
	2-hydroxy-5,6-dihydronaphthalene-1-carboxylic acid	
	(Z)-3-hydroxyacrylic acid	
	2-formylbenzoic acid	
	benzaldehyde	
	malealdehyde	
	2-hydroxy-1-naphthoic acid	[92]
	2-formylbenzoic acid	
	3,4-dihydroxybenzoic acid	
	2-hydroxybenzoic acid	
Pyrene	1,6-pyrenequinone	[93]
	1,8-pyrenequinone	
	phenanthrene-4,5-dicarbaldehyde	
Anthracene	anthrone	[88]
	1,8-dihydroxy-9(10H)-anthracenone	
	9,10-anthraquinone	
	2-hydroxy-9,10-anthracenedione	
	1,4-dihydroxy-9,10-anthracenedione	
	1,2-benzenedicarboxaldehyde	
	9,10-anthraquinone	[91]
	3-hydroxy-2-naphthoic acid	
	naphthalene	
	benzene	
	malealdehyde	
	(Z)-4-oxobut-2-enoic acid	
	6-octadecanoic acid	[90]
	15-hydroxypentadecanoic acid	
	hexane-1,2,3-trimethoxy	
Benz[a]anthracene	mono-hydroxy benz[a] anthracene	[94]
	(E)-2-hydroxy- 3-(2-hydroxyanthracen-1-yl)acrylic acid	
	naphthalene-2,3-dicarboxylic acid	
	naphthalene-1,4-diol	
	(E)-2-(2-carboxyvinyl)benzoic acid	
Benzo[a]pyrene	benzo(a)pyrene-4,5-epoxide	[43,95]
	benzo(a)pyrene-4,5-diol	
	4-Chrysenol	
	benzo(a)pyrene-7-ol	
	benzo(a)pyrene-7,8-diol	
	benzo(a)pyrene-7,8,9,10-tetraol	
	pyrene	
	phthalic acid, butyl isohexyl ester	
	ethyl 3-hydroxybenzoate	

separation from the liquid. Submerged photocatalysts may not utilize light energy effectively. This limitation can reduce their usage and potentially cause secondary environmental pollution. A new approach in photocatalyst synthesis is the development of lightweight floating photocatalysts which not only facilitate the recycling of catalysts but also allow for direct illumination in aqueous solutions, thereby effectively increasing light capture [96]. Additionally, the easy recovery of used photocatalysts for subsequent processes helps avoid secondary pollution and reduces process costs. Various floating photocatalysts have been constructed on floating carriers such as expanded perlite, high-surface-area vermiculite, fly ash cenospheres, low-density polyethylene, and others [97,98].

There are described the various methods for immobilizing photocatalysts on floating materi-

als, including sol-gel, dip coating, spray coating, solvothermal, hydrothermal, liquid-phase deposition, sol-carbonization, surface modification, centrifugation, and 3D printing [99]. Besides the simple methodology for obtaining floating particles, the system effectively utilizes UV photoactivation, as it ensures the availability of TiO_2 at the water/air phase boundary. Easy separation from the treated solution and the possibility of recycling make it a promising photocatalyst.

In a study [100] a floating water photocatalyst consisting of TiO_2 deposited using a direct deposition method on perlite granules was synthesized and characterized. The resulting black TiO_2 foams which can float on water extend the photoreaction range from ultraviolet to visible light and demonstrate excellent solar-driven photocatalytic activity and long-term stability for the complete mineralization of floating insoluble hexadecane and some typical pesticides. This performance surpasses that of commercial TiO_2 Degussa P25 under AM 1.5 irradiation.

Floating alginate beads, obtained by crosslinking a sodium alginate solution containing TiO_2, organobentonite (NaOB), and $CaCO_3$ with Ca^{2+} in an acidified solution (CH_3COOH), demonstrated that the addition of 1% NaOB improved thermal stability and facilitated the adsorption process, thereby enhancing photocatalytic activity [101,102]. The floating adsorbent-photocatalyst exhibited good stability, retaining up to 80% of its dye decolorization capability even after seven reuse cycles. Anusuyadevi et al. [103] developed a floating Pickering photocatalyst carrier based on green cellulose nanofibers (CNF) derived from wood. The metal-free semiconductor photocatalyst, g-C_3N_4, was easily embedded within the foam by mixing the photocatalyst with an air bubble suspension, followed by casting and drying to form a solid foam. The resulting photocatalytic foams floated on water for 4 weeks. Under mild irradiation conditions and without stirring the g-C_3N_4-CNF floating nanocomposite foam has removed nearly three times more dye than pure g-C_3N_4 powder after 6 hours.

Currently, we have found only one study with real application of a floating photocatalyst for water purification from PAHs in oil sands tailings ponds. The floating photocatalyst used was a composite material made of microbubble glass powder and TiO2 nanoparticles (particle diameter 25 nm). After 21 hour of UV irradiation at 365 nm with 50 W UV-LED lamp the PAHs concentration was decreased by 89% [104].

To date, the floating photocatalysts for PAHs remediation present an intriguing alternative as they maximize light utilization and surface aeration enhancing pollutant removal efficiency and reducing subsequent treatment costs.

Conclusions

Heterogeneous photocatalysis is evidently the most promising method for converting PAHs into less harmful compounds or achieving their complete mineralization in aqueous environments. Researchers are currently focusing on enhancing the efficiency of photocatalysts when using solar energy to degrade persistent organic pollutants.

The main approaches include chemical modification and the creation of heterojunction catalysts. Doping nanoparticles with metals or non-metals can reduce the band gap of the semiconductor, create additional active sites on the surface, thus increasing the number of generated radicals and reducing the recombination rate of electron-hole pairs, which contributes to more efficient degradation of pollutants. Semiconductor materials with heterojunctions are characterized by better separation of photogenerated electrons and holes, reducing charge recombination, which is critical for improving photocatalytic efficiency. These two approaches significantly enhance the properties of photocatalysts and form the basis for developing new highly efficient materials for PAH degradation. However, for the development of reliable and efficient technologies for the photocatalytic decomposition of organic pollutants, including PAHs, a deeper understanding of the mechanisms and kinetics of photodegradation processes is required.

However, to develop reliable and efficient technologies for the photocatalytic degradation of organic pollutants, including PAHs, a deeper understanding of the mechanisms and kinetics of photodegradation processes is required. A particularly promising direction could be the development of porous photocatalytic materials capable of remaining suspended or floating on the water surface for extended periods, thereby more effectively utilizing solar energy. It is also worth noting that almost all known studies on the photocatalytic degradation of PAHs have been conducted only under laboratory conditions, so the issue of creating specialized reac-

tors for scaling up this purification technology remains a subject for future studies.

Acknowledgement

This research was supported by National Academy of Sciences of Ukraine, project #0124U002973.

The authors express their gratitude to the brave Armed Forces of Ukraine for defending our country, enabling us to conduct scientific research in the city of Kharkiv.

References

1. Lawal, A. T. *Cogent Environ. Sci.* **3**, 1 (2017).
2. Li R., Cai J., Li J. et al. *J. Hazard. Mater.* **423**, 127065 (2022).
3. Abdel-Shafy, H. I. & Mansour, M. S. M. *Egypt. J. Pet.* **25**, 107 (2016).
4. Marris, C. R., Kompella, S. N. Miller, M. R. et al. *J. Physiol.* **598**, 227 (2020).
5. International Agency for Research on Cancer. *Some Non-Heterocyclic Polycyclic Aromatic Hydrocarbons and Some Related Exposures*. (International Agency for Research on Cancer, Lyon, 2010).
6. U.S. DEPARTMENT OF HEALTH AND HUMAN SERVICES. Toxicological Profile for Polycyclic Aromatic Hydrocarbons (PAHS). *ATSDR's Toxicol. Profiles* (2002).
7. Commission Regulation. *Off. J. Eur. Union.* **2016**, 48 (2018).
8. European Commission. *Off. J. Eur. Union* **119**, 103 (2023).
9. US EPA. *NATIONAL PRIMARY DRINKING WATER REGULATIONS*. (US EPA, 2014).
10. Keith, L. H. *Polycycl. Aromat. Compd.* **35**, 147 (2015).
11. Health Canada. *Maximum Levels for Chemical Contaminants in Foods*. (2016).
12. Mojiri, A., Zhou, J. L., Ohashi, A. et al. *Sci. Total Environ.* **696**, 133971 (2019).
13. Yang B., Shi Y., Xu S. et al. *Environ. Sci. Process. Impacts* **24**, 32 (2022).
14. Patel, A. B., Shaikh, S., Jain, K. R. et al. *Front. Microbiol.* **11**, (2020).
15. Dobaradaran S., Schmidt Torsten C., Lorenzo-Parodi Nerea et al. *Environ. Pollut.* **259**, 113916 (2020).
16. Gbeddy, G., Goonetilleke, A., Ayoko, G. A. et al. *Environ. Pollut.* **257**, 113510 (2020).
17. Barreca S., Oliveri, I. P., Lo Presti F. et al. *Sep. Purif. Technol.* **348**, 127516 (2024).
18. Sher, S., Waseem, M., Leta, M. K. *Environ. - MDPI* **10**, 1 (2023).
19. Lamichhane, S., Bal Krishna, K. C., Sarukkalige, R. *Chemosphere* **148**, 336 (2016).
20. Amin Mojiri, Zhou, John L. Ohashi, Akiyoshi. *SCIENCE OF THE TOTAL ENVIRONMENT* **696**, 133971 (2019).
21. Singh, R., Singh, P., Tripathi, S., Chandra, K. K. & Bhadouria, R. *Xenobiotics in Urban Ecosystems: Sources, Distribution and Health Impacts*. (2023).
22. Haritash, A. K. & Kaushik, C. P. *J. Hazard. Mater.* **169**, 1 (2009).
23. Abdel-Fatah, M. A. *Ain Shams Eng. J.* **9**, 3077 (2018).
24. Boulkhessaim, S., Gacem A. K., Samreen H. et al. *Nanomaterials* **12**, 1 (2022).
25. Ibhadon, A. O. & Fitzpatrick, P. *Catalysts* **3**, 189 (2013).
26. Kukkar, D., Kukkar, P., Younis, S. A. & Kim, K. H. *J. Clean. Prod.* **333**, 130026 (2022).
27. Monteiro, F. C., Guimaraes, I. D. L., de Almeida Rodrigues, P. et al. *J. Photochem. Photobiol. A Chem.* **437**, (2023).
28. Kolahalam L. A., Kasi Viswanath, I. V., Diwakar Bhagavathula S. et al. *Mater. Today Proc.* **18**, 2182 (2019).
29. Chen, X. & Mao, S. S. *Chem. Rev.* **107**, 2891 (2007).
30. Khan N. A., Khan S. U., Ahmed S. et al. *Asian J. Water, Environ. Pollut.* **16**, 81 (2019).
31. Kisch, H. *Characterization of Solid Materials and Heterogeneous Photocatalysis and Water Photoinitiators for Polymer Applied Homogeneous*. (2015).
32. Pichat, P. *Photocatalysis and Water Purification: From Fundamentals to Recent Applications*. (2013).
33. Kunduru K. R., Nazarkovsky M., Shady F. et al. *Water Purification,* **33**, 33-74 (2017).
34. Nasir, A., Khalid, S., Yasin, T. & Mazare, A. *Energies* **15**, (2022).
35. Zhang, J., Zhou, P., Liu, J. & Yu, J. *Phys. Chem. Chem. Phys.* **16**, 20382 (2014).
36. Landmann, M., Rauls, E. & Schmidt, W. G. *J. Phys. Condens. Matter* **24**, (2012).
37. Mahlambi, M. M., Ngila, C. J. & Mamba, B. B. *Journal of Nanomaterials,* 2015 (2015).
38. T.A.Khalyavka, S.V.Camyshan, L.A.Davydenko et al. *Funct. Mater.* **25**, 067 (2018).
39. Hurum, D. C., Agrios, A. G., Gray, K. A. et al. *J. Phys. Chem. B* **107**, 4545 (2003).
40. Durodola S. S., Olaniran K. Ore, Odunayo T. et al. *J. Fluoresc.* **34**, 501 (2024).
41. Gusain, R., Gupta, K., Joshi, P. & Khatri, O. P. *Advances in Colloid and Interface Science* **272**, 102009 (2019).

42. Liu, Z., Liu, X., Lu, Q. et al. *J. Taiwan Inst. Chem. Eng.* **96**, 214 (2019).
43. Bai, H., Zhou, J., Zhang, H. & Tang, G. *Colloids Surfaces B Biointerfaces* **150**, 68 (2017).
44. Luo Z. H., Wei C. L., He N. N. et al. *J. Nanomater.* **2015**, (2015).
45. Rachna, Rani, M. & Shanker, U. *J. Environ. Manage.* **248**, 109340 (2019).
46. Zhao, Z. & Omer, A. A. *Env. Sci. Pol. Res.* **27,** 17530–17540 (2019).
47. Cheng K., Cai Z., Fu J. et al. *Chem. Eng. J.* **358**, 1155 (2019).
48. Sun X., He W., Hao X. et al. *J. Hazard. Mater.* **412**, 125221 (2021).
49. Daneshvar, N., Salari, D. & Khataee, A. R. *J. Photochem. Photobiol. A Chem.* **162**, 317 (2004).
50. Minh Huong L., Minh Dat N., Thanh Hoai N. et al. *Environmental Nanotechnology, Monitoring and Management*. **22**, 100966 (2024).
51. Islam, S. Z., Nagpure, S., Kim, D. Y. & Rankin, S. E. *Inorganics* **5**, 15 (2017).
52. Azmi R., Hwang S., Yin W. et al. *ACS Energy Lett.* **3**, 1241 (2018).
53. Chudinovych O.V., Myroniuk D.V., Myroniuk L.A. et al. *Funct. Mater.* **30**, 171 (2023).
54. Nga, P. T. T., Duc, N. M., Van Minh, N. & Lien, N. H. *Vietnam J. Chem.* **60**, 389 (2022).
55. Liu, Q., Li, X., Wan, Z., Xu, D. & Liu, C. *Colloids Surfaces A Physicochem. Eng. Asp.* **700**, 134765 (2024).
56. Vela, N., Martínez-Menchón, M., Navarro, G. et al. *J. Photochem. Photobiol. A Chem.* **232**, 32 (2012).
57. Sliem, M. A., Salim, A. Y. & Mohamed, G. G. *Vol. 371, Pages 327 - 335* **371**, 327 (2019).
58. Rachna, Rani, M. & Shanker, *J. Photochem. Photobiol. A Chem.* **381**, (2019).
59. Batchamen Mougnol, J. B., Waanders, F., Ntwampe, S. K. O. et al. *Environ. Syst. Res.* **11**, 25 (2022).
60. Chauhan H. A., Rafatullah M. A., Khozema A. et al. *J. Water Process Eng.* **47**, 102714 (2022).
61. Manna, M., Sen, S. *Appl. Surf. Sci.* **630**, (2023).
62. Tandorn, S., Lamkhao, S., Thiraphatchotiphum C. et al. *Chem. Eng. J.* **457**, 141190 (2023).
63. Zhao J., Tian W., Chu M. *et al. Chemosphere* **297**, 134175 (2022).
64. Dai Y., Wang Y., Zuo G. et al. *Chemosphere* **293**, (2022).
65. Dai, Y. Wang Y., Zuo G. et al. *Appl. Surf. Sci.* **572**, (2022).
66. Wang Y., Feng W., Gong A. et al. *Catal. Letters* **154**, 3574 (2024).
67. Marques M., Cervello D., Mari M. et al. *Polycycl. Aromat. Compd.* **40**, 524 (2020).
68. Ali A., Raza T., Adeel F. et al. *Synth. Met.* **287**, (2022).
69. Al-Hunaiti, A., Ghazzy, A. M., Mahmoud, N. T. *Chem. Eng. J. Adv.* **19**, (2024).
70. Li, T., Wang, M., Hao, Y. *Sci. Total Environ.* **857**, (2023).
71. Yang G., Jiang Y., Yin B. et al. *Environ. Sci. Pollut. Res.* **30**, 70260 (2023).
72. Qiao, M., Fu, L. & Barcelo, D. *Process Saf. Environ. Prot.* **159**, 376 (2022).
73. Huang R., Zhang M., Zheng Z. et al. *NANOMATERIALS* **11**, (2021).
74. Lu J., Guo Z., Li M. et al. *Chemosphere* **318**, (2023).
75. Brindhadevi K., Kim T P, Sulaiman A. et al. *Environ. Res.* **252**, (2024).
76. Karam F. F., Hussein F. H., Baqir S. J. et al. *Int. J. Photoenergy* **2014**, 1 (2014).
77. Soni, H., Kumar, N., Patel, K. & Kumar, R. N. *Polycycl. Aromat. Compd.* **40**, 257 (2020).
78. Saloot, M. K., Borghei, S. M. & Shirazi, R. H. S. M. *Desalin. Water Treat.* **220**, 287 (2021).
79. Ji H., Liu W., Sun F. et al. *Chem. Eng. J.* **419**, (2021).
80. Al-Madanat, O., Alsalka, Y., Dillert, R. et al. *Catalysts* **11**, 1 (2021).
81. Quynh, T. X. & Toan, V. D. *Ecol. Environ. Conserv.* **28**, 606 (2022).
82. McQueen A. D., Ballentine M. L., May L. R. et al. *ACS Environ. Sci. Technol. Water* **2**, 137 (2022).
83. Zhang J., Yu F., Ke X. et al. *Molecules* **27**, (2022).
84. Alomairy, S., Gnanasekaran, L., Rajendran, S. & Alsanie, W. F. *Chemosphere* **343**, 140274 (2023).
85. Meenu, N., Rani, M. & Shanker, U. *Environ. Sci. Adv.* **3**, 249 (2023).
86. Martínez-Vargas B. L., Cruz-Ramírez M., Díaz-Real J. A. et al. *J. Photchem. Photobiol. A: Chemistry*, **369**, 85 (2019).
87. Guo Y., Dai Y., Zhao W. et al. *Appl. Catal. B Environ.* **237**, 273 (2018).
88. Woo, O. T., Chung, W. K., Wong, K. H. et al. *J. Hazard. Mater.* **168**, 1192 (2009).
89. Fu J., Kyzas G. Z., Cai Z. et al. *Chem. Eng. J.* **335**, 290 (2018).
90. Theerakarunwong, C. D. & Phanichphant, S. *Water. Air. Soil Pollut.* **229**, (2018).
91. Shanker, U., Jassal, V. & Rani, M. *J. Environ. Manage.* **204**, 337 (2017).
92. Rachna, Rani, M. & Shanker, U. *Chem. Eng. J.* **348**, 754 (2018).
93. Yang X., Cai H., Bao M. et al. *Chem. Eng. J.* **334**, 355 (2018).

94. Rachna, Rani, M. & Shanker, U. *J. Photochem. Photobiol. A Chem.* **381**, 111861 (2019).
95. Kudlek, E. & Dudziak, M. *Water Sci. Technol.* **77**, 2407 (2018).
96. Darkhosh, F., Lashanizadegan, M., Mahjoub, A. R. & Cheshme Khavar, A. H. *Solid State Sci.* **91**, 61 (2019).
97. Zhang L., Xing Z., Zhang H. et al. *Appl. Catal. B Environ.* **180**, 521 (2016).
98. Długosz, M., Waś, J., Szczubiałka, K. & Nowakowska, M. *J. Mater. Chem. A* **2**, 6931 (2014).
99. Nasir A. M., Jaafar J., Aziz F. et al. *J. Water Process Eng.* **36**, (2020).
100. Zhang K., Zhou W., Zhang X. et al. *Appl. Catal. B Environ.* **206**, 336 (2017).
101. Dalponte Dallabona, I., Mathias, Á. L. & Jorge, R. M. M. *Colloids Surfaces A Physicochem. Eng. Asp.* **627**, (2021).
102. Ferreira, A. V. de T. P. F., Barbosa L. V., de Souza S. D. et al. *J. Photochem. Photobiol. A Chem.* **419**, 113483 (2021).
103. Anusuyadevi, P. R., Riazanova, A. V, Hedenqvist et al. *ACS Omega* **5**, 22411 (2020).
104. Bleasdale-Pollowy, A., Chan, C., Leshuk, T. M. C. & Gu, F. *Environ. Technol. Innov.* **33**, 103492 (2024).